

MOLECULAR DYNAMICS SIMULATION OF TENSILE DEFORMATION OF NANOMETER MULTILAYER Cu/Ta MATERIALS

MOLEKULARNO DINAMSKO SIMULACIJE NATEZNO DEFORMIRANIH NANOMETERSKIH VEČPLASTNIH MATERIALOV NA OSNOVI BAKRA IN TANTALA

Hu Jianian^{1, 2}, Zhang Haotian², Zhu Youlin³, Li Peibo³, Luo Guoqiang^{1,3,*},
Wang Chuanbin^{1,3}, Shen Qiang^{1,3}, Zhang Lianmeng^{1,3}

¹Chaozhou Branch of Chemistry and Chemical Engineering Guangdong Laboratory, Guangdong, Chaozhou, China

²State Key Laboratory of Precision Blasting, Jiangnan University, Hubei, Wuhan, China

³State Key Laboratory of Advanced Technology for Materials Synthesis and Processing, Wuhan University of Technology, Hubei, Wuhan, China

Prejem rokopisa – received: 2022-05-26; sprejem za objavo – accepted for publication: 2022-07-04

doi:10.17222/mit.2022.505

In this research, the tensile mechanical properties and microstructure evolution of Cu/Ta nanolayered composites were studied using the molecular dynamics simulation method. By analyzing the tensile stress/strain relationship of Cu/Ta with different interface structures and the movement of dislocations during the stretching process, the deformation mechanism of materials with different interface structures and the effect of interface structures on the tensile strength of Cu/Ta nanolayered composites are revealed. The effect of shear localization during extension is also analyzed. The results show that the dislocation structures at the interfaces of Kurdjumov-Sachs-type and Nishiyama-Wasserman-type samples are parallelogram and triangular interface defect arrays, respectively, which can easily induce two Shockley partial dislocations to slide along different {111} planes, forming an intersection and merging into ladder-rod dislocations. However, dislocations between the Kurdjumov-Sachs {112}-type sample interfaces exhibit parallel array characteristics, while the interfacial dislocations have non-planar interface components, which can induce deformation twinning. The process is dissociated through a set of intrinsic interfacial dislocations. Shockley partial dislocations are then formed by dislocation motion, creating stacking faults (SF₁), and then the second set of partial dislocations may nucleate from the interface and slide on the adjacent SF₁ plane, eventually forming deformation twinning.

Keywords: molecular dynamics simulation, Cu/Ta nanolayered composites, tensile properties, deformation mechanism, dislocation motion

Avtorji opisujejo natezne mehanske lastnosti in razvoj mikrostrukture večplastnih Cu/Ta nano-kompozitov s pomočjo metod molekularno-dinamske simulacije. Z analiziranjem zveze med natezno napetostjo in deformacijo Cu/Ta z različno strukturo mejnih ploskev in gibanjem dislokacij med procesom raztezanja so avtorji odkrili kakšen je deformacijski mehanizem materialov z različno strukturo mejnih ploskev in njihov vpliv na natezno trdnost večplastnih Cu/Ta nano-kompozitov. Ugotavljali so kakšen je deformacijski mehanizem in vpliv lokaliziranega striga med raztezanjem. Rezultati raziskave kažejo na to, da so strukture vzorcev dislokacij na mejnih ploskvah Kurdjumov-Sachsovega in Nishiyama-Wassermanovega tipa s tri- in štirikotno ureditvijo napak na mejnih ploskvah. To lahko enostavno sproži (inducira) dve Shockleyjevi parcialni dislokaciji, ki zdrsita vzdolž različnih {111} ravnin in tvorita presečišče dislokacij z obliko zložljivih lestev. Vendar vzorci dislokacij Kurdjumov-Sachsovega {112}-tipa na mejnih ploskvah kažejo značilno vzporedno razporeditev. Pri tem imajo mejne dislokacije neplanarne (neravninske oz. 3d) komponente, ki lahko inducirajo deformacijo z dvojčenjem. Proces poteka z razdruževanjem vrste notranjih mejnih dislokacij. Pri tem nastajajo Shockleyjeve parcialne dislokacije, ki tvorijo napake zloga (SF₁). Nato lahko nastane (nukleira) še drugi set parcialnih dislokacij na mejnih ploskvah in zdrs na sosednje SF₁ ravnine, kar lahko privede do deformacije z dvojčenjem.

Ključne besede: molekularno-dinamske simulacije, večplastni nanokompoziti Cu/Ta, natezna deformacija, mehanske lastnosti, gibanje dislokacij

1 INTRODUCTION

Tantalum has excellent properties, such as high melting point, high strength and good wear resistance, while copper exhibits high thermal conductivity, excellent mechanical properties and good electrical conductivity.¹⁻⁴ Therefore, in recent years, nanometer Cu/Ta multilayer related reports on composite materials (MNCs) have become a hotspot of academic research.^{5,6} Copper/tantalum

nanocomposites combine the advantages of Ta and Cu and have a wide range of applications in the electronics industry, used for semiconductor and superconductor fabrication, optical and magnetic systems, etc. Combinations of PVD, cross accumulation rolling (CARB) and intermediate annealing steps are the most commonly used techniques for the preparation of nanostructured Cu/Ta MNCs and bulk Cu/Ta nanolayered multilayers.⁷⁻⁹ However, the nanostructure of Cu/Ta MNCs prepared with these methods is not uniform, the thickness is uncontrollable and the preparation cost is high.¹⁰ With the

*Corresponding author's e-mail:
hujianian1@outlook.com (Hu Jianian)

rapid development of simulation technology, the use of molecular dynamics simulation technology to calculate and optimize the parameters of the nano/macrostructure and discover the evolution mechanism of the microstructure during the deformation process has become an important tool for the study of metal nanocomposites.¹¹

Grain boundaries of MNCs are important for the material properties such as strength, fracture, work hardening and damage evolution under irradiation and impact.^{12,13} R. Bejaud et al.¹⁴ revealed that the Cu-Ag interface directly or indirectly induces the nucleation of twinning dislocations through Lomer dislocations, and through an atomic-scale analysis, they revealed that twinning is a common plasticity mechanism. Lu et al.¹⁵ studied the effect of the Al/Cu MNC interface stress on the dislocation nucleation and propagation law during deformation and established a model of the interface stress, dislocation nucleation and motion parameters in an analytical form. The study shows that the yield and failure of Al/Cu MNCs are mainly controlled by the evolution of dislocations in the Al and Cu layers, respectively. Due to the interactions between stacking faults and dislocations, Al(100)/Cu(100), the shear strength of the MNCs decreases with decreasing the repeating interlayer spacing.

Interfacial microstructure characteristics of MNCs are important for their mechanical properties, such as interfacial defects, modulation period, interfacial structure, dislocation nucleation and deformation twinning nucleation.¹⁶ Lu et al.¹⁷ used molecular dynamics (MD) simulations to investigate the effect of interfacial structures such as interfacial defects and modulation period (λ) on the deformation mechanism of Cu/Ta nanometallic multilayers (MNCs) under uniaxial stretching. The results show that the Cu(111)/Ta(110) interface is the initial site of dislocation nucleation, hindering further diffusion of dislocation motion toward the interface. During the tensile process involving Cu/Ta MNCs, the maximum stress decreases with the increase in λ , and there is a critical point where the flow strength of the MNCs is the largest. However, the effects of interfacial dislocation nucleation and deformation twinning nucleation on the mechanical properties of Cu/Ta MNCs are lacking.

Interfacial dislocation nucleation and deformation twinning nucleation are closely related to the interfacial orientation of nanolayered multilayer films.¹⁸ Zhang et al.¹⁹ investigated the nucleation of lattice dislocations at the Cu/Nb interface with the Kurdjumov-Sachs (KS) orientation relationship using atomic-scale simulations, sys-

tematically explored the possibilities for the slip system, and concluded that, contrary to the initial design, the location nucleation sites of misfits correlate poorly with pre-existing misfit dislocations. Beyerlein et al.²⁰ investigated the effect of the intrinsic bimetallic interface structure on lattice dislocation nucleation. It was found that the interface structure has a great influence on dislocation nucleation and the type of nucleation sites. At the same time, it was found that interfacial dislocations with non-planar Burgers vectors can prevent interfacial sliding, and the interface is more prone to twinning nucleation.

Therefore, in this research, the MD method was used to study the influence of the interface structure of Cu/Ta materials with different orientation relationships on the mechanical properties. Interface structure characteristics of the three interface orientations were compared, and the effects of the interface structure and stretching direction on the deformation mechanism were discussed. In this research, we studied the deformation mechanism of Cu/Ta nanolayered composites, emphasizing how the interface structure affects the interaction with defects, the strengthening mechanisms of samples with different interface structures and the effect of the loading direction on the mechanical properties of the samples.

2 COMPUTATIONAL DETAILS

2.1 General

We selected three kinds of Cu/Ta nanolayered composites with classical interface structure orientations. The interface structures included the Kurdjumov-Sachs type (KS), Nishiyama-Wasserman type (NW) and Kurdjumov-Sachs {112} type (KS{112}). Their crystal orientations and box sizes are shown in **Table 1**. The molecular dynamics simulation used in this research was LAMMPS. The simulation process first used the conjugate gradient (CG) method to obtain the minimum equilibrium energy model. The model optimization-process energy and force-pause tolerances were 10^{-7} eV/nm and 10^{-13} eV/nm, respectively. The simulation calculations of the tensile deformation of Cu/Ta MNCs were performed within the NpT ensemble, the temperature was controlled by the Nose-Hoover system, and the pressure was controlled by uniaxial stretching of the box along the z-axis direction. The calculation results of MD were post-processed by the OVITO visualization software. By identifying the crystal lattice types and structural defects in atomic crystals, the microstructure evolution process

Table 1: Cu/Ta MNCs with Kurdjumov-Sachs, Nishiyama-Wasserman and KS {112} interface orientations

Interface Constituent	KS		NW		KS{112}	
	Cu layer	Ta layer	Cu layer	Ta layer	Cu layer	Ta layer
Lx	114 [0 1 -1]	102 [-1 1 -1]	115 [0 1 -1]	89 [0 0 1]	114 [-1 1 0]	102 [1 1 -1]
Ly	64 [-12 1 1]	35 [-2 -1 1]	58 [-2 1 1]	55 [1 -1 0]	44 [1 1 -1]	35 [1 -1 0]
Lz	12 [1 1 1]	11 [0 1 1]	12 [1 1 1]	11 [1 1 0]	[1 1 2]	[1 1 2]

and deformation mechanism of the Cu/Ta MNCs under tensile deformation were analyzed.²¹

2.2 Interfacial structure characteristics

Figure 1 shows side views of the interface structures after the relaxation equilibrium of the three models. Atomic lattice types were identified using the common neighbor analysis algorithm (CNA) in OVITO. In this figure, green, blue and red areas stand for FCC, BCC and HCP structural coordination atoms, respectively, while white ones stand for the "unknown or non-standard" structural atoms caused by high lattice distortion. It can be seen that all three model interfaces are sharp. The interfaces of the KS and NW samples are flat. In contrast, the interface of the KS{112}-type sample is non-planar, containing regular facets (white atoms in **Figure 1c**). At the same time, parallel out-of-plane stacking faults (red atoms in **Figure 1c**) are observed in the KS{112}-type sample.

The interface organization structures of the three interface models are shown in **Figure 2**. They were identified using polyhedral template matching (PTM) in OVITO. The results show that the interface defects of the KS sample form periodic parallelogram arrays, and that the defect regions (red HCP atoms) are located at the four corners of the parallelogram. The NW-type sam-

ple-interface defect array is parallel and rod-shaped along the $[0\ 1\ -1]$ direction, and the whole is a periodic triangle. The KS{112}-type sample interface contains parallel and discontinuous HCP and FCC coordination lines. The dislocations at the interface cannot be identified by the dislocation extraction algorithm (DXA) so that the Thompson tetrahedron is required to identify them. The results show that the KS-type sample interface contains two sets of $b_1 = 1/2[0\ 1\ -1]$ and $b_2 = 1/2[1\ 0\ -1]$ types of total dislocations along the CA and CB trajectories, respectively (**Figure 2a**). The interfacial dislocation type of the NW-type sample is a partial dislocation, and the Burgers vector is $[2\ -1\ -1]$ (shown as b_3 in **Figure 2b**). The interface of the in-plane component of the misfit dislocation of the KS{112}-type sample is $b_4 = 1/2[1\ -1\ 0]$ (shown as b_4 in **Figure 2c**), and the out-of-plane component is $b = 1/6[1\ 1\ 2]$ (**Figure 1b**). The interfacial structures of the three models have different characteristics that affect dislocation nucleation and deformation during their stretching.

3 RESULTS

Figure 3 shows the stress-strain curves of the Cu/Ta nanolayered composites with different interface structures under the tensile load at 300 K. It can be seen from the figure that the stress increases linearly with the strain

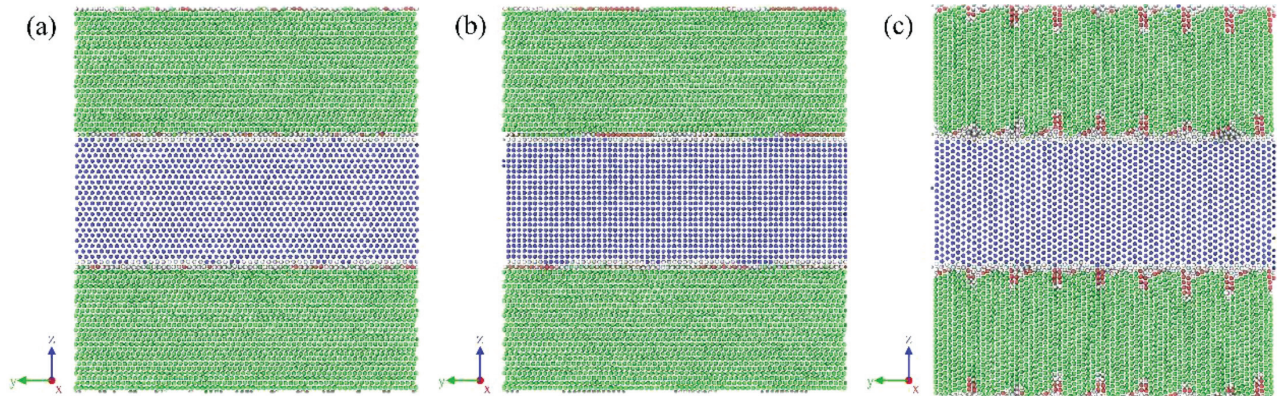


Figure 1: Geometric models of the samples after relaxation: a) KS type, b) NW type, c) KS {112} type

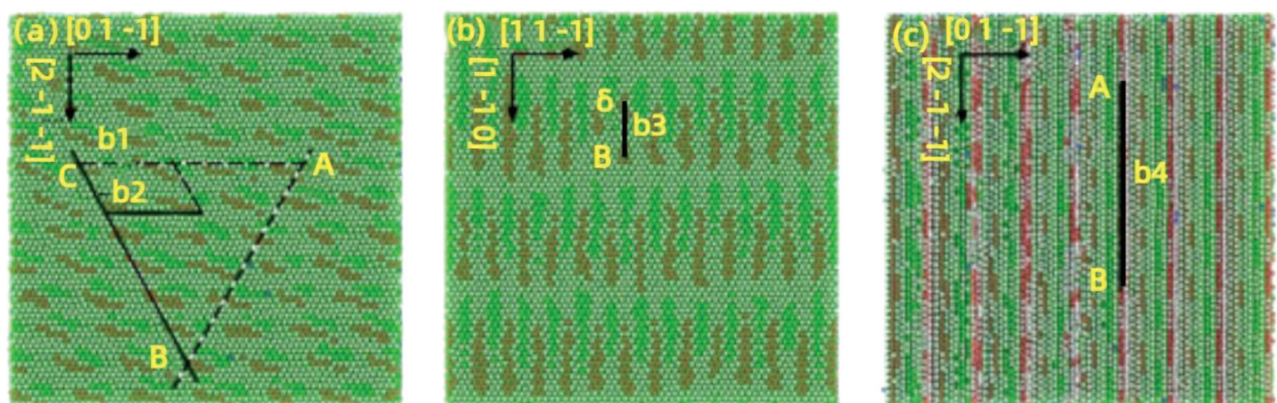


Figure 2: Atomic structures of the interfaces identified with PTM: a) KS, b) NW, c) KS{112}

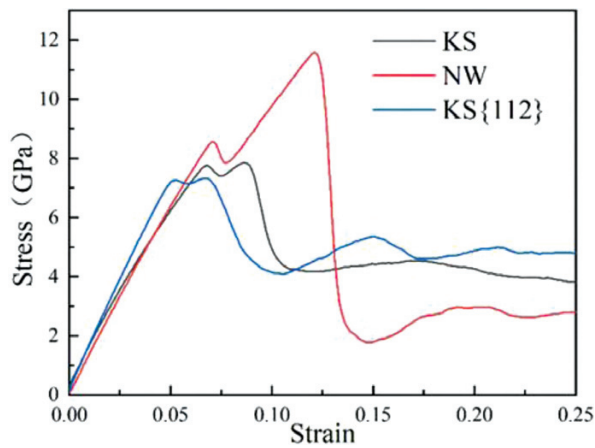


Figure 3: Stress-strain curves of Cu/Ta MNCs with different interface structures under tensile loading

until the first peak, which is the yield point of the Cu layer. Then the stress decreases over a small segment and begins to increase linearly until the second peak when the Ta layer yields and plastic deformation begins. The yield strength (the first peak), highest strength (the second peak) and mean flow strength of the three interface structures are shown in **Table 2**. It can be seen from the table that the KS{112} type sample has the highest flow strength, followed by the KS type sample, while the NW type sample has the lowest flow strength.

Table 2: Yield strength, maximum strength and average flow strength of the three interfacial-structure samples

Interface	Loading orientation	σ_{yield} (GPa)	σ_{max} (GPa)	σ_{flow} (GPa)
KS	$\langle 112 \rangle_{\text{Cu}}$	7.75	7.85	4.22
NW	$\langle 112 \rangle_{\text{Cu}}$	8.56	11.58	2.62
KS{112}	$\langle 111 \rangle_{\text{Cu}}$	7.25	7.32	4.81

To explore the differences between the tensile mechanical behaviors of the three samples of interface structures, this section studies the evolution law of microscopic defects of the three samples during the tensile process. The microscopic defects at the yield point of Cu/Ta MNC Cu layers with three different interfacial

structures are shown in **Figure 4**. To observe the change in the defect microstructure, the FCC and BCC structure atoms of the undeformed Cu layer and Ta layer are deleted here. In all the samples, the Shockley partial dislocation (the green line in **Figure 4**, the Burgers vector is $1/6p$) nucleation was observed on the Cu-layer side of the interface and in the form of partial dislocation loops along the $\{111\}$ plane. The slip plane diffuses within the Cu layer, leaving an internal stacking fault (SF). In the KS-type Cu/Ta MNCs, before the Cu layer yields, part of the dissociated misfit dislocations diffuse in the Cu layer along the $\{111\}$ slip plane parallel to the z-axis direction, forming stacking faults penetrating the Cu layer. In the NW-type Cu/Ta MNCs, in addition to $1/6p$, the formation of stepped rod dislocations (the red line in **Figure 4**, the Burgers vector is $1/6n$ dislocation) was also observed. But for the KS{112}-type Cu/Ta MNCs, the balanced interface structure contains dissociative misfit dislocations, extending into the Cu layer, resulting in a lower activation barrier for dislocation nucleation at the interface. Therefore, at lower strain and stress, the formation of partial dislocation loops is first observed in the Cu layer.

To release the stress and accommodate the strain, more Shockley partial dislocations nucleate and extend from the interface into the Cu layer. As the strain increases, the Shockley dislocation density increases, while the stress decreases for a short time.²² The snapshots of the microscopic defects of the three samples at the first peak-valley point are shown in **Figure 5**. Under this strain, part of the Shockley dislocation loop moves along the $\{111\}$ slip plane to the other side of the interface, and the front segment of the dislocation loop annihilates, leaving only dislocation lines on both sides of the stacking fault. As the critical stress of the unit dislocation loop transport across the interface in the confinement layer model is higher than the critical stress of dislocation loop bending, and due to the difference between the geometric slip systems of the Cu and Ta layers, the dislocations at the interface cannot be transboundary and the planar dislocation transport is therefore blocked at the interface. According to **Figure 5**, sessile Lomer-

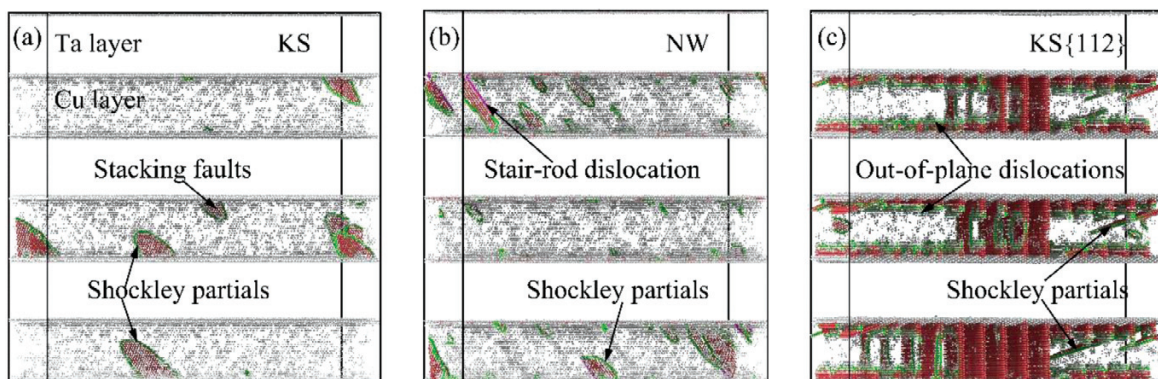


Figure 4: Snapshots of microscopic defects at the yield point of Cu layer: a) KS-type sample, $\epsilon = 0.065$, b) NW-type sample, $\epsilon = 0.069$, c) KS {112}, $\epsilon = 0.048$

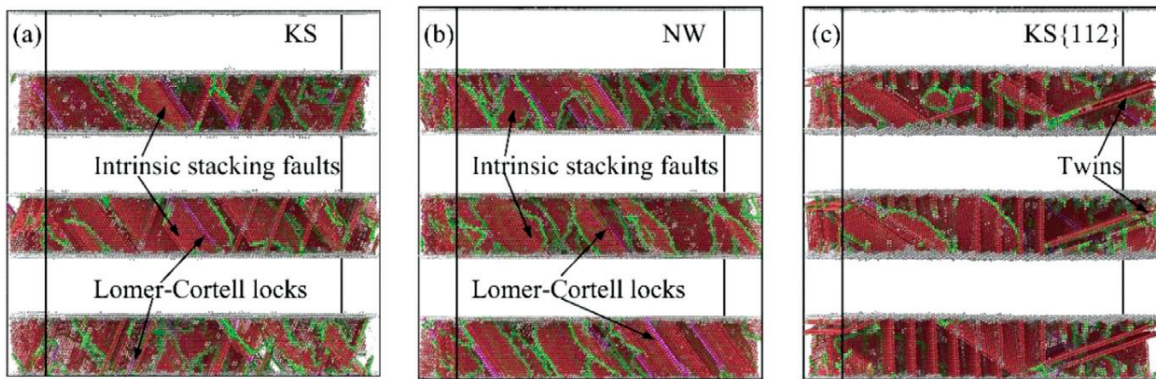


Figure 5: Snapshots of microscopic defects in the samples: a) KS-type sample, $\epsilon = 0.074$, b) NW-type sample, $\epsilon = 0.077$, c) KS{112}, $\epsilon = 0.058$

Cortell (LC) locks appear in the KS and NW-type samples, while twinning is observed in the KS{112}-type sample. This indicates that the interfacial structure may affect the formation of dislocations and defects in the Cu layer, thereby affecting the way of plastic deformation.

Due to the higher yield strength of Ta, dislocations in the Cu layer are blocked at the interface. Due to the weak interfacial shear, the shear stress field generated by the dislocations close to the interface traps the slip dislocations at the interface, so the dislocation density decreases and the stress rises to the second peak point. **Fig-**

ure 6 shows snapshots of the microscopic defects at the second stress peak (the yield point of the Ta layer). Ta layer yielding is divided into three stages: interfacial shear, accompanied by the movement of lattice dislocations in the interface plane; dislocation loop nucleation with concomitant interfacial structural compression; finally, dislocations escape from the interface by overcoming the attraction within the interface layer. At the same time, it can be seen that the interface forms a $1/2\alpha$ dislocation loop on the Ta-layer side.

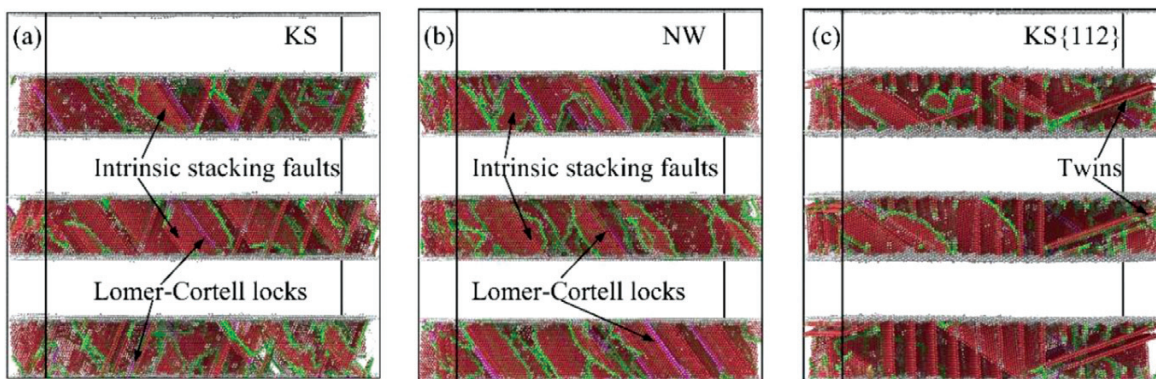


Figure 6: Snapshots of microscopic defects at the yield point of the Ta layer: a) KS-type sample, $\epsilon = 0.086$, b) NW-type sample, $\epsilon = 0.121$, c) KS {112}, $\epsilon = 0.068$

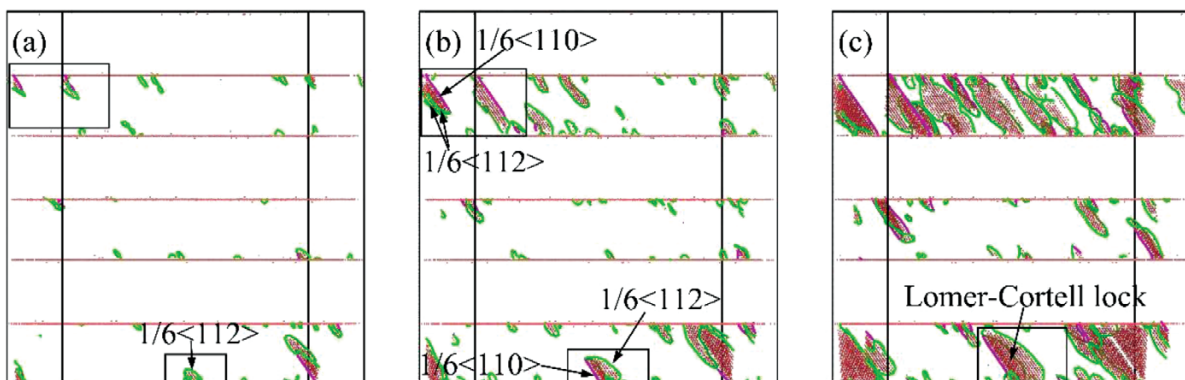


Figure 7: Snapshots of defective microstructures during the formation of the Lomer-Cortell (LC) lock in the NW-type samples: a) $\epsilon = 0.068$, b) $\epsilon = 0.069$, c) $\epsilon = 0.070$

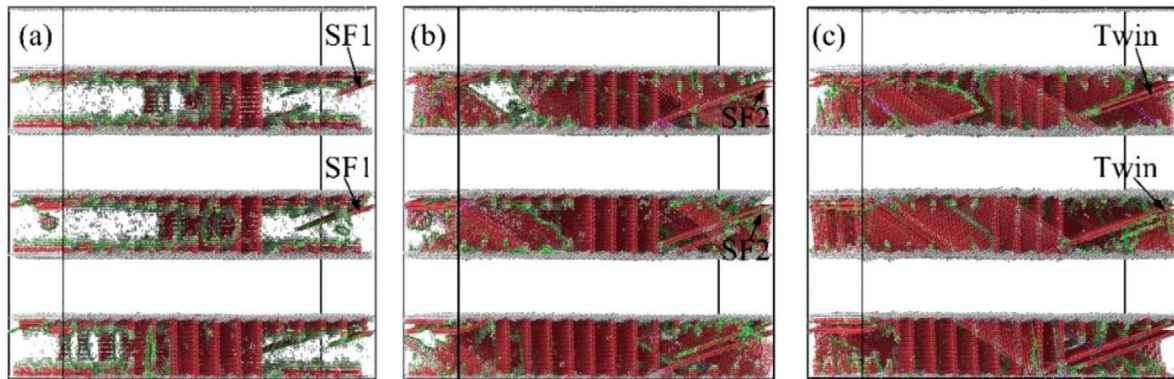
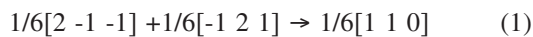


Figure 8: Snapshots of defective microstructures of the twist formation in the KS {112} type samples: a) $\varepsilon = 0.048$, b) $\varepsilon = 0.054$, c) $\varepsilon = 0.060$

Figure 7 shows the formation of sessile Lomer-Cortell (LC) locks in the NW-type samples.^{23,24} When the strain is 0.068, the interface forms a Shockley partial dislocation loop on the Cu-layer side (**Figure 7a**, the Burgers vector is $1/6p$). As the leading portion slips, an intrinsic stacking fault is formed in the slip region. Due to the intersection of the two dominant partial dislocations on the $\{111\}$ plane, their motion is hindered and they merge to form ladder-rod dislocations. The merging process can be expressed with the following reaction formula:



The stepped rod dislocation is located at the intersection of two different stacking faults where the Burgers vector is $1/6n$ and the slip plane is $\{100\}$. Such dislocations cannot slide into the Cu layer and hinder the dislocation motion, thereby enhancing the mechanical properties of the material. Two intersecting stacking faults form their Shockley partial dislocations and, in turn, sessile stepped rod dislocations at the intersections form sessile Lomer-Cortell (LC) locks.

Figure 8 shows microscopic defect snapshots of the twin formation in the KS{112}-type samples. The unique interfacial structure of the KS{112}oCu||{112}nTa interface induced twinning due to the existence of a non-planar interface component and out-of-plane Burgers vector component of the interfacial dislocation. When $\varepsilon = 0.048$, the interfacial dislocations dissociate, and each dislocation decomposes into residual dislocations and Shockley partial dislocations extend into the Cu layer. Subsequently, the Shockley dislocation partially slips along the $\{111\}$ slip plane to form a stacking fault (SF₁) (**Figure 8a**). A single layer of stacking faults cannot form twins, but it is the prerequisite for the formation of twins. The sliding of Shockley partial dislocations on adjacent planes creates twinning in FCC metals.²⁵ So when the interval between SF₁ is small enough, the number of Shockley branches that subsequently need to be nucleated is reduced. On the contrary, when SF₁ is separated, the twins are more difficult to be excited, because, from the energy point of view, it is difficult for the twins to nucleate in large numbers. When $\varepsilon = 0.054$, in

the region adjacent to SF₁, the second group of partial dislocations begins to nucleate and extend from the interface to the Cu layer (**Figure 8b**), resulting in a slippage on the $\{111\}$ plane adjacent to the first fault, while the sliding surface is parallel to SF₁. As the strain increases, another stacking fault (SF₂) forms near the first one; they are twinned when the strain in the region between SF₁ and SF₂ is 0.06 (**Figure 8c**). Unlike dislocation slip, deformation twinning largely changes the lattice orientation of the grains and forms adjacent boundaries between the twin orientation and the original lattice orientation. The twin interface acts as a substantial barrier to dislocation transport, preventing dislocation slippage.²⁶

There are out-of-plane dislocation defects and parallel defect arrays at the interface of the KS{112} type samples, so the nucleation dislocations tend to slip onto the parallel slip plane, and the Shockley partial dislocation motions are mostly of the first and second types. The interface of the KS-type and NW-type samples is a parallelogram or triangular defect array, and most of the nucleating dislocations move on different slip planes, but some Shockley dislocations tend to move more towards the third and fourth types.

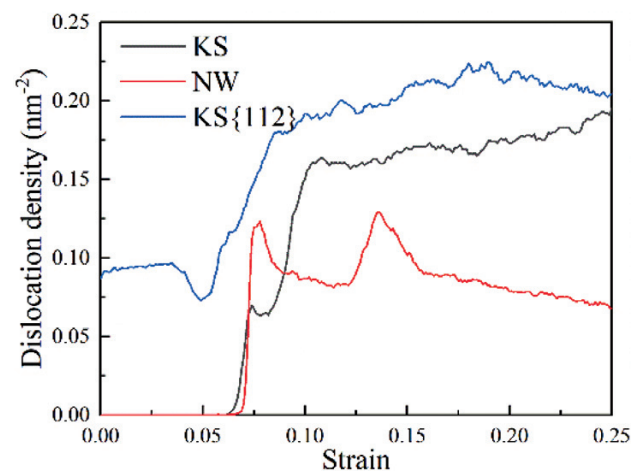


Figure 9: Curves of dislocation density evolution with strain for the three interface structure samples

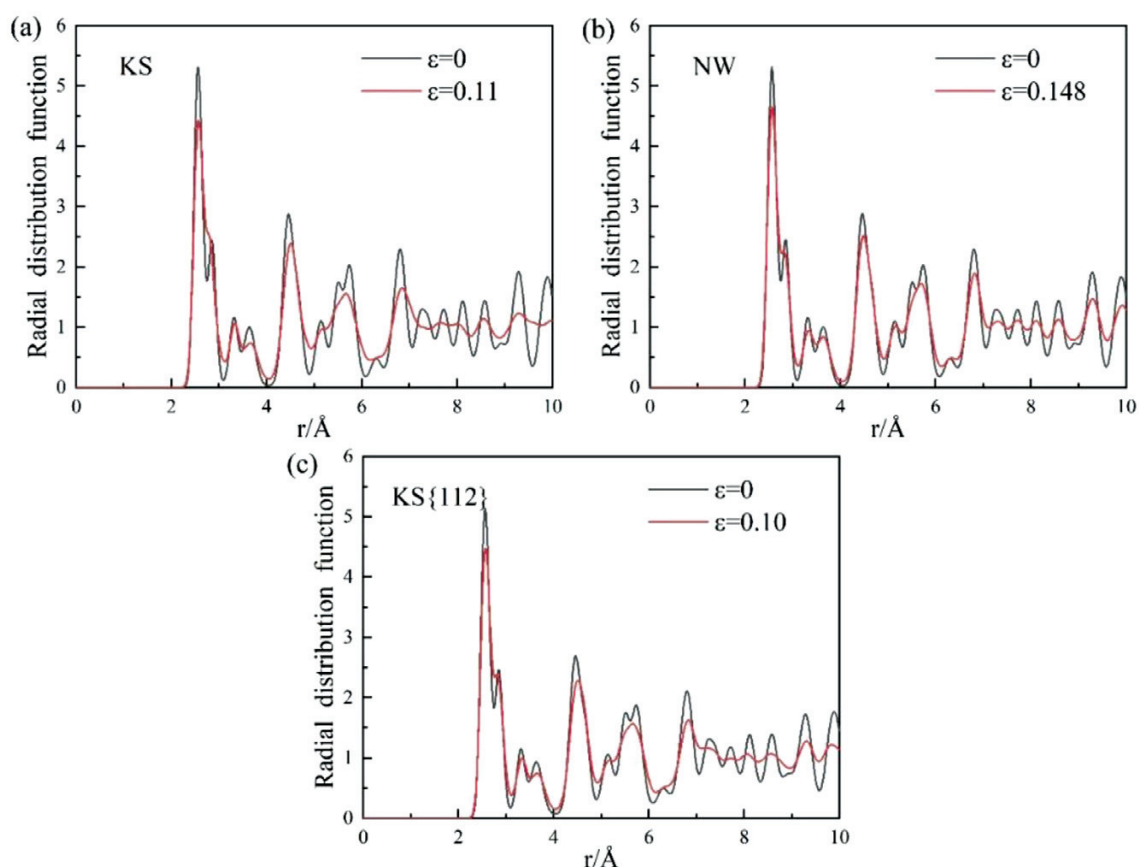


Figure 10: Radial distribution function curves before and after deformation of the samples with three interfacial structures

Figure 9 shows the evolution curves of dislocation density with strain in the samples with three interface structures. The dislocation density change is roughly divided into three stages according to the deformation process. The first stage is the elastic deformation stage. The dislocation density of the KS and NW samples is zero, while that of the KS{112} sample is not zero due to out-of-plane dislocations. Before the Cu layer of the sample yields, some out-of-plane dislocations are parallel to the z-axis. The expansion of the {111} plane and the breaking of out-of-plane dislocations lead to a decrease in the dislocation density. The second stage is the yielding stage, where the yielding of the Cu layer leads to a rapid increase in the dislocation density, which leads to a decrease in the stress until the first peak and valley. During the first and second peaks of stress, the dislocation density decreases. This is because the dislocations close to the interface are trapped by the interface and some dislocations are annihilated due to the interactions of dislocations. After the Ta layer yields, the dislocation density increases rapidly. The third stage is the plastic deformation stage. The proliferation rate and disappearance rate of dislocations in the matrix tend to be in dynamic equilibrium, and the dislocation density tends to be stable.²⁷

To reveal more details of the plastic deformation mechanism of the Cu/Ta MNCs with three interfacial

structures, **Figure 10** shows the corresponding radial distribution functions before and after deformation. It can be seen that the peak intensities of the three curves before and after deformation all decrease, and some long-range peaks disappear, indicating that the order of the samples decreases after deformation. For the KS and NW-type samples, the orderly decrease in the strength is attributed to the generation of dislocation and stacking fault defects, while for the KS{112}-type samples, the formation of twins is also a reason for the decrease in the strength.²⁸

4 CONCLUSION

In this paper, the deformation mechanism of Cu/Ta nanolayered composites with different interface structures was studied; the interaction between the interface structure and defect structure and the strengthening methods for the samples with different interface structures were revealed. The main conclusion is that the KS{112} type sample interface is a parallel defect array, and the interface dislocation has a non-planar interface component, which induces deformation twinning. The formation of deformation twinning starts with the dissociation of intrinsic interfacial dislocations into Shockley partial dislocations, followed by the formation of SF₁ by dislocation motion; then, the second set of partial dislo-

cations may nucleate from the interface and slide on the adjacent SF₁ plane, and finally deformation twins are formed. The interface structures of the KS-type and NW-type samples are parallelogram and triangular interface defect arrays, respectively, which can easily induce two Shockley partial dislocations to slide along different (111) planes, intersect and form stepped rod dislocations.

Acknowledgements

This research was supported by the Guangdong Provincial Key Field Research and Development Program (Grant No.: 2021B0707050001), and the scientific research team (Project No. HJL202202A007) of the Chaozhou Branch of the Guangdong Laboratory of Chemistry and Fine Chemicals (Hanjiang Laboratory).

5 REFERENCES

- A. M. Abyzov, F. M. Shakhov, A. I. Averkin, V. I. Nikolaev, Mechanical properties of a diamond-copper composite with high thermal conductivity, *Materials & Design*, 87 (2015), 527–539, doi:10.1016/j.matdes.2015.08.048
- Z. L. Pan, Y. L. Li, Q. Wei, Tensile properties of nanocrystalline tantalum from molecular dynamics simulations, *Acta Materialia*, 56 (2008) 14, 3470–3480, doi:10.1016/j.actamat.2008.03.025
- Q. X. Pei, C. Lu, F. Z. Fang, H. Wu, Nanometric cutting of copper: A molecular dynamics study, *Computational Materials Science*, 37 (2006) 4, 434–441, doi:10.1016/j.commatsci.2005.10.006
- J. H. Qin, Q. Chen, C. Y. Yang, Y. Huang, Research process on property and application of metal porous materials, *Journal of Alloys and Compounds*, 654 (2016) 39–44, doi:10.1016/j.jallcom.2015.09.148
- K. A. Darling, E. L. Huskins, B. E. Schuster, Q. Wei, L. J. Kecskes, Mechanical properties of a high strength Cu-Ta composite at elevated temperature, *Materials Science and Engineering A: Structural Materials: Properties, Microstructure and Processing*, 638 (2015), 322–328, doi:10.1016/j.msea.2015.04.069
- A. S. Tran, T. H. Fang, Size effect and interfacial strength in nanolaminated Cu/Cu_xTa_{100-x} composites using molecular dynamics, *Computational Materials Science*, 184 (2020), doi:10.1016/j.commatsci.2020.109890
- L. F. Zeng, R. Gao, Q. F. Fang, X. P. Wang, Z. M. Xie, S. Miao, T. Hao, T. Zhang, High strength and thermal stability of bulk Cu/Ta nanolamellar multilayers fabricated by cross accumulative roll bonding, *Acta Materialia*, 110 (2016), 341–351, doi:10.1016/j.actamat.2016.03.034
- G. P. Zhang, F. Liang, X. M. Luo, X. F. Zhu, A review on cyclic deformation damage and fatigue fracture behavior of metallic nanolayered composites, *Journal of Materials Research*, 34 (2019) 9, 1479–1488, doi:10.1557/jmr.2019.22
- X. Q. Liang, J. Y. Zhang, Y. Q. Wang, S. H. Wu, F. Zeng, K. Wu, G. Liu, G. J. Zhang, J. Sun, Tuning the size-dependent He-irradiated tolerance and strengthening behavior of crystalline/amorphous Cu/Ta nanostructured multilayers, *Materials Science and Engineering: A*, 672 (2016), 153–160, doi:10.1016/j.msea.2016.07.005
- X. Y. Zhu, J. T. Luo, F. Zeng, F. Pan, Microstructure and ultrahigh strength of nanoscale Cu/Nb multilayers, *Thin Solid Films*, 520 (2011) 2, 818–823, doi:10.1016/j.tsf.2010.12.251
- H. Yavas, A. Fraile, T. Huminiuc, H. S. Sen, E. Frutos, T. Polcar, Deformation-Controlled Design of Metallic Nanocomposites, *ACS Applied Materials and Interfaces*, 11 (2019) 49, 46296–46302, doi:10.1021/acsami.9b12235
- T. Fu, X. Peng, S. Weng, Y. Zhao, F. Gao, L. Deng, Z. Wang, Molecular dynamics simulation of effects of twin interfaces on Cu/Ni multilayers, *Materials Science and Engineering: A*, 658 (2016), 1–7, doi:10.1016/j.msea.2016.01.055
- S. Weng, H. Ning, N. Hu, C. Yan, T. Fu, X. Peng, S. Fu, J. Zhang, C. Xu, D. Sun, Y. Liu, L. Wu, Strengthening effects of twin interface in Cu/Ni multilayer thin films – A molecular dynamics study, *Materials & Design*, 111 (2016), 1–8, doi:10.1016/j.matdes.2016.08.069
- R. Béjaud, J. Durinck, S. Brochard, Twin-interface interactions in nanostructured Cu/Ag: Molecular dynamics study, *Acta Materialia*, 144 (2018), 314–324, doi:10.1016/j.actamat.2017.10.036
- C. Lv, J. Yang, X. P. Zhang, Y. Cai, X. Y. Liu, G. J. Wang, S. N. Luo, Interfacial effect on deformation and failure of Al/Cu nanolaminates under shear loading, *Journal of Physics D: Applied Physics*, 51 (2018) 33, doi:10.1088/1361-6463/aad2a8
- S. Srinivasan, C. Kale, B. C. Hornbuckle, K. A. Darling, M. R. Chancey, E. Hernandez-Rivera, Y. Chen, T. R. Koenig, Y. Q. Wang, G. B. Thompson, K. N. Solanki, Radiation tolerance and microstructural changes of nanocrystalline Cu-Ta alloy to high dose self-ion irradiation, *Acta Materialia*, 195 (2020), 621–630, doi:10.1016/j.actamat.2020.05.061
- L. Lu, C. Huang, W. L. Pi, H. G. Xiang, F. S. Gao, T. Fu, X. H. Peng, Molecular dynamics simulation of effects of interface imperfections and modulation periods on Cu/Ta multilayers, *Computational Materials Science*, 143 (2018), 63–70, doi:10.1016/j.commatsci.2017.10.034
- M. A. Bhatia, M. Rajagopalan, K. A. Darling, M. A. Tschopp, K. N. Solanki, The role of Ta on twinnability in nanocrystalline Cu-Ta alloys, *Materials Research Letters*, 5 (2017) 1, 48–54, doi:10.1080/21663831.2016.1201160
- R. F. Zhang, J. Wang, I. J. Beyerlein, T. C. Germann, Dislocation nucleation mechanisms from fcc/bcc incoherent interfaces, *Scripta Materialia*, 65 (2011) 11, 1022–1025, doi:10.1016/j.scriptamat.2011.09.008
- I. J. Beyerlein, J. Wang, K. Kang, S. J. Zheng, N. A. Mara, Twinnability of bimetal interfaces in nanostructured composites, *Materials Research Letters*, 1 (2013) 2, 89–95, doi:10.1080/21663831.2013.782074
- A. Stukowski, V. V. Bulatov, A. Arsenlis, Automated identification and indexing of dislocations in crystal interfaces, *Modelling and Simulation in Materials Science and Engineering*, 20 (2012) 8, doi:10.1088/0965-0393/20/8/085007
- P. A. Gruber, E. Arzt, R. Spolenak, Brittle-to-ductile transition in ultrathin Ta/Cu film systems, *Journal of Materials Research*, 24 (2009) 6, 1906–1918, doi:10.1557/jmr.2009.0252
- D. Choudhuri, A. CampBell, Interface dominated deformation mechanisms in two-phase fcc/B2 nanostructures: Nishiyama-Wasserman vs. Kurdjumov-Sachs interfaces, *Computational Materials Science*, 177 (2020), doi:10.1016/j.commatsci.2020.109577
- Z. G. Yan, Y. J. Lin, Lomer-Cottrell locks with multiple stair-rod dislocations in a nanostructured Al alloy processed by severe plastic deformation, *Materials Science and Engineering A: Structural Materials: Properties, Microstructure and Processing*, 747 (2019), 177–184, doi:10.1016/j.msea.2019.01.066
- M. Hosseini, N. Pardis, H. D. Manesh, M. Abbasi, D. I. Kim, Structural characteristics of Cu/Ti bimetal composite produced by accumulative roll-bonding (ARB), *Materials & Design*, 113 (2017), 128–136, doi:10.1016/j.matdes.2016.09.094
- C. B. Wang, J. J. Wang, J. N. Hu, S. L. Huang, Y. Sun, Y. L. Zhu, Q. Shen, G. Q. Luo, Shear Localization and Mechanical Properties of Cu/Ta Metallic Nanolayered Composites: A Molecular Dynamics Study, *Metals*, 12 (2022) 3, doi:10.3390/met12030421
- B. B. He, B. Hu, H. W. Yen, G. J. Cheng, Z. K. Wang, H. W. Luo, M. X. Huang, High dislocation density-induced large ductility in deformed and partitioned steels, *Science*, 357 (2017) 6355, 1029–1032, doi:10.1126/science.aan0177
- L. Lu, Y. F. Shen, X. H. Chen, L. H. Qian, K. Lu, Ultrahigh strength and high electrical conductivity in copper, *Science*, 304 (2004) 5669, 422–426, doi:10.1126/science.1092905